iScience

CellPress
OPEN ACCESS

Article

Diya – A universal light illumination platform for multiwell plate cultures

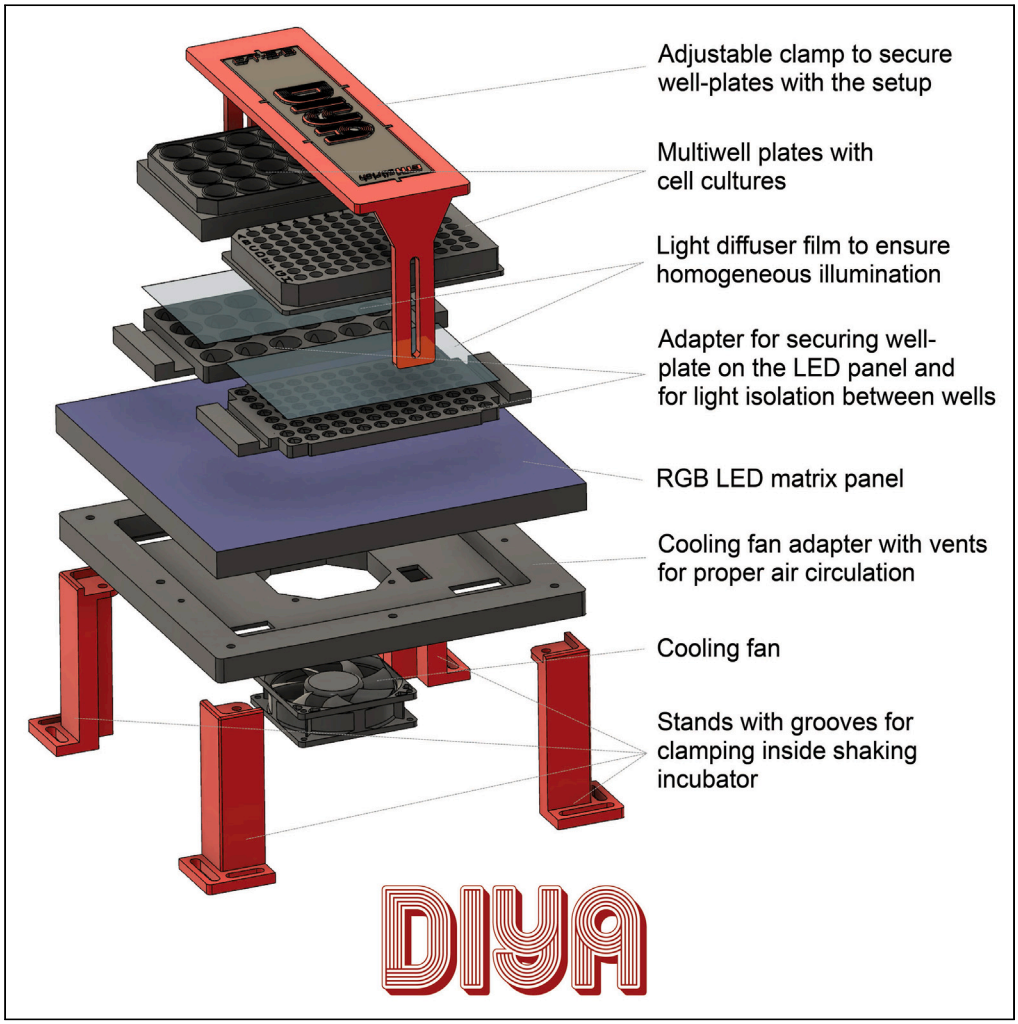

Sant Kumar, Stanislav Anastassov, Stephanie K. Aoki, ..., Peter Buchmann, Paul Argast, Mustafa Khammash

mustafa.khammash@bsse.ethz.ch

Highlights

Light illumination apparatus compatible with different cell culture plates/dishes

Ensures viable conditions for (bacterial, yeast, human) cells under light stimulation

Demonstration: Activation of different optogenetic systems in different cell lines

Demonstration: Optogenetic setpoint tuning of *in vivo* antithetic integral controller

Kumar et al., iScience 26, 107862
October 20, 2023
https://doi.org/10.1016/j.isci.2023.107862

iScience

CellPress
OPEN ACCESS

Article

Diya – A universal light illumination platform for multiwell plate cultures

Sant Kumar,[1,2] Stanislav Anastassov,[1,2] Stephanie K. Aoki,[1] Johannes Falkenstein,[1] Ching-Hsiang Chang,[1] Timothy Frei,[1] Peter Buchmann,[1] Paul Argast,[1] and Mustafa Khammash[1,3,*]

SUMMARY

Recent progress in protein engineering has established optogenetics as one of the leading external non-invasive stimulation strategies, with many optogenetic tools being designed for *in vivo* operation. Characterization and optimization of these tools require a high-throughput and versatile light delivery system targeting micro-titer culture volumes. Here, we present a universal light illumination platform – Diya, compatible with a wide range of cell culture plates and dishes. Diya hosts specially designed features ensuring active thermal management, homogeneous illumination, and minimal light bleedthrough. It offers light induction programming via a user-friendly custom-designed GUI. Through extensive characterization experiments with multiple optogenetic tools in diverse model organisms (bacteria, yeast, and human cell lines), we show that Diya maintains viable conditions for cell cultures undergoing light induction. Finally, we demonstrate an optogenetic strategy for *in vivo* biomolecular controller operation. With a custom-designed antithetic integral feedback circuit, we exhibit robust perfect adaptation and light-controlled set-point variation using Diya.

INTRODUCTION

In an expanding repertoire of synthetic biology tools, optogenetics is leading the charge as one of the most precise strategies for external stimulation of *in vivo* processes. Inspired by natural photosynthesis phenomena, optogenetics entails influencing cellular processes with light.[1,2] Features like excellent spatial localization together with precise temporal and quantitative control render light advantageous over other stimulation techniques such as chemical induction.[3] *In vivo* engineering of photosensors, photoreceptors, and other light-sensitive mechanisms has led to the development of several optogenetic tools,[4–8] along with their utility in gene expression regulation,[4] protein-protein interaction[9] as well as many other applications. The sheer numbers of these tools and their diversity have led to the initiation of an ever-expanding online database.[10] Optogenetics is envisioned to assist a multitude of advanced applications including developmental biology research,[11,12] bioproduction,[13,14] tissue engineering,[15,16] biomaterials,[17,18] and *in vivo* controller circuit design and prototyping,[19] among many others.

Employing optogenetic strategies for synthetic biology applications is not possible without suitable light delivery technologies. Progress in the field of optogenetics has also propelled the research and development of several light induction hardware-software schemes,[20] which we will refer to as optogenetic platforms in this article. According to the application specific requirements, these platforms have been custom-designed to enable optogenetic induction at different scales, from microscopic single cell stimulation to large bioreactor bulk culture induction. Although the microscopic light induction technologies[21,22] facilitate optogenetic studies requiring resolutions up to intracellular levels, their throughput is extremely limited for bulk population studies. Medium[23–25] and large bioreactor[26–28] options are suitable for biotechnology and bioprocessing applications, with some setups also facilitating continuous culture operation.[24] However, experiments on these platforms demand considerable resources such as culture medium, and are also limited in throughput.

Characterization and optimization studies for optogenetic tools and downstream genetic circuits require high throughput and iterative experimentation cycles. Multiwell plate illumination devices[29–34] are suitable for these applications as they enable parallel induction of tens of individual wells, each with culture volume within a range of hundreds of micro-liters. Some of these setups, e.g.,[30] provide illumination with no optical separation between wells limiting the number of independent conditions one can apply in a light induction experiment. Although some other previously proposed setups such as optoPlate-96,[33] light plate apparatus (LPA),[31] and light activation at variable amplitudes (LAVA)[34] ensure optical isolation between neighboring wells in their design, they are custom-designed for specific multiwell types and sizes, thus limiting their utility in diverse culture conditions. Furthermore, the construction/assembly of these devices requires expertise in reasonably advanced mechatronic tools and engineering, which is usually not available in basic biology labs. Some commercial ready-to-use

[1]Department of Biosystems Science and Engineering (D-BSSE), ETH Zürich, Mattenstrasse 26, 4058 Basel, Switzerland
[2]These authors contributed equally
[3]Lead contact
*Correspondence: mustafa.khammash@bsse.ethz.ch
https://doi.org/10.1016/j.isci.2023.107862

platforms (e.g. Lumos from Axion Biosystems) exist but they are substantially expensive. A recent design proposed by Höhener et al.[35] overcame these limitations by using an affordable off-the-shelf LED matrix panel with closely spaced LEDs. This panel allows for the light induction of multiwell plates and culture dishes with different shapes and sizes with an easy-to-assemble and easy-to-program framework. However, due to appreciably high heat generation (cell culture temperature reaching over 40°C) during constant light induction experiments, this setup is limited to lower duty-cycle pulsed-width modulated induction, and is not suitable for continuous light operation. It also does not include safeguards for light bleedthrough in neighboring wells, and is not operable in shaking cell culture incubators.

To overcome the limitations of the available state-of-the-art multiwell plate light induction platforms, we present a universal multiwell plate light illumination device — Diya. Using a high density RGB LED matrix panel, its design is compatible for cell culture illumination in different multiwell plate types and culture dishes. Diya includes a simple but effective active thermal management system allowing for continuous and sustained light induction operation. It guarantees uniform/homogeneous illumination within wells, minimal illumination variability between wells with the same input, robust optical isolation between neighboring wells, three light wavelengths for induction, and supports static as well as dynamic, that is, time-varying induction experiments. It also offers safeguards for operation in shaking cell culture incubators. We have also custom-developed an intuitive graphic user interface (GUI) making the programming of light induction experiments on Diya a simple and effortless experience, which requires no coding skills. Diya achieves all these features with an affordable (< USD 200), easy-to-assemble and easy-to-build hardware design, thus reducing barriers for pursuing optogenetics research in basic biology labs with fewer resources and limited engineering competence.

In this work, we fully characterize and validate the proposed Diya platform with technical analyses, such as temperature and uniformity analysis, as well as with diverse light induction experiments. We demonstrate the versatility of this platform by successfully reproducing multiple results in the synthetic biology literature involving state-of-the-art optogenetic tools (Opto-T7,[36] EL222,[37] CRY2PHR-CIB1,[38] GAVPO,[39] and CcaS-CcaR[23,40]) in multiple model organisms (bacteria, yeast and human cell lines).

Finally, we demonstrate the power of our approach through a case study involving advanced biomolecular circuit designs. We experimentally illustrate how optogenetics, facilitated by the Diya setup, can be utilized to rapidly vary reaction rates within complex *in vivo* controllers. Inspired by classical engineering disciplines, the application of control theory in synthetic biology is becoming increasingly prevalent. In recent years, many biomolecular controller motifs involving chemical reaction networks have been proposed, built and analyzed.[41–47] One of the more elaborate genetic circuits, which has gained widespread attention from biologists and engineers, is the antithetic integral feedback (AIF) controller.[48] This controller motif has been demonstrated to achieve set-point tracking with respect to a given output molecule even in the presence of external disturbances and in inherently noisy cellular environment[43] — a feature known as robust perfect adaption (RPA). Previous *in vivo* implementations of this motif involved circuit designs requiring plasmid copy number variation[41,42] or external chemical induction[43,47] for tuning controller parameters such as the controller set-point. Plasmid copy numbers can vary substantially between cells, and chemical inducers can degrade or get metabolized by the cells. These shortcomings limit the effective control over the chemical network reaction rates, that is, the controller parameters. Optogenetics can be employed to overcome these limitations. In addition to providing precise (temporal, spatial and quantitative) stimulation pathway, this technique also enables us to vary the controller parameters reversibly, which can be challenging with other methodologies. In this study, we have designed an *in vivo* optogenetic AIF controller by enabling light control over the sensing reaction rate. Access to this reaction rate allows closure of the AIF loop as well as precise control over the set-point. Using this circuit design and the Diya platform, we successfully managed to vary the output of interest, without compromising the RPA properties. This approach enables a high-throughput screening through the parameter (sensing reaction rate) space by simply applying different light intensities in parallel.

RESULTS

Diya – Hardware design and operation protocol

Diya is an optogenetic platform for cells cultured in multiwell plates or other culture dishes. Central to Diya is a high density RGB LED matrix panel having 64x64 RGB LEDs with 3 mm pitch, which allows symmetric alignment of multiple LEDs under each well in a standard multiwell plate with up to 96 wells. Thus, it supports light induction of cells cultured in clear-bottom multiwell plates (up to 96 wells) or culture dishes by placing the plate on the panel such that the panel LEDs underneath each well act as separate light illumination sources. Two standard multiwell plates can be simultaneously accommodated on the panel for parallel light induction experiments (Figures 1A and 1B). The RGB LEDs provide illumination capability with three different wavelengths of light centered around 622 nm (red), 520 nm (green), and 464 nm (blue), by LED panel design specifications. An expanded view of all the components in a Diya setup is illustrated in Figure 1A. The operation protocol of this platform is discussed further in the next section, and shown in Figure 1C.

Diya incorporates 3D-printed adapters for different multiwell plates, which secure the cell culture plate on the panel in the correct alignment (Figure 1A). The adapters are designed with gridded protrusions on their base that can latch between LEDs on the panel. These well plate adapters also help in optical isolation of neighboring wells to avoid light spillover (Figure S2). We have designed these adapters for standard 6-, 24-, and 96-well plates, and the design files are provided with this article. During optogenetic experiments, a diffuser film/paper can also be sandwiched between the adapter and the well plate leading to uniform/homogeneous illumination of each well. The coefficient of variation between the captured pixel intensities within a single illuminated well is observed to be less than 0.1 (Figures 2A and 2B), confirming homogeneous illumination within wells. Besides, the lower coefficient of variation (< 0.1) in the mean pixel intensities of the captured images of all wells implies that the same digital input leads to a similar light illumination intensity in different wells across the LED panel (Figures 2C and 2D).

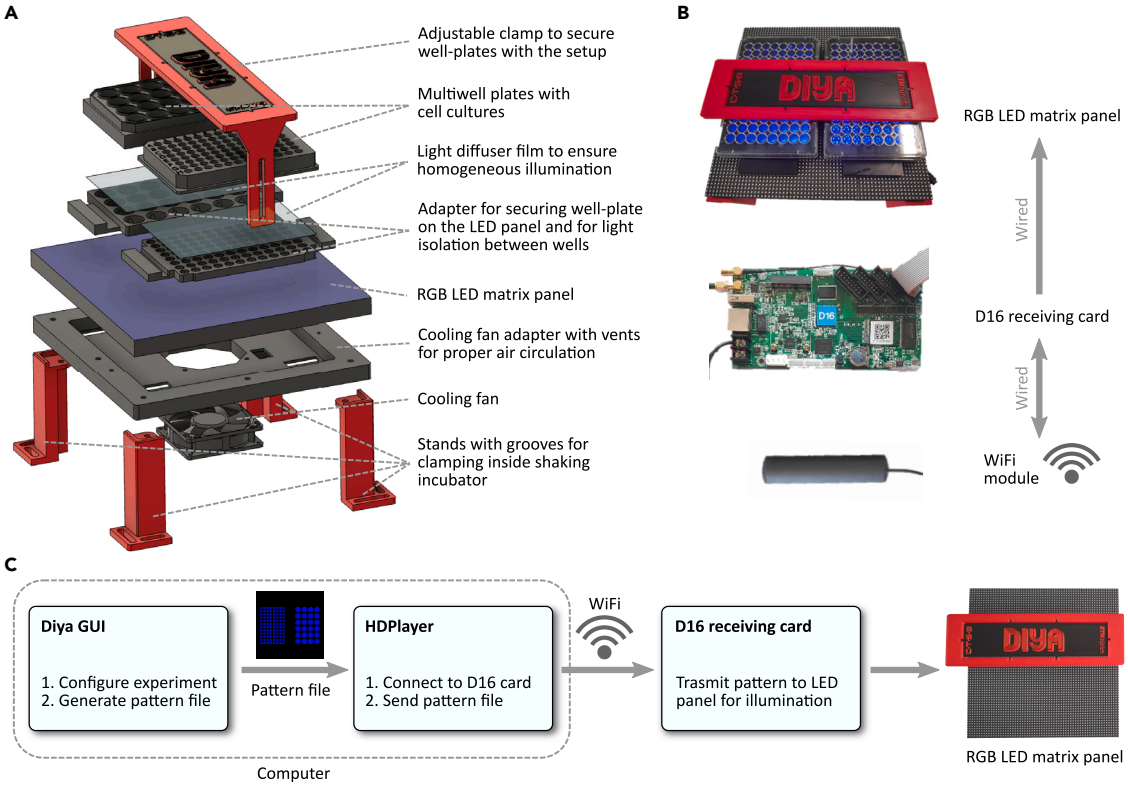

Figure 1. Diya hardware and operation protocol

(A) An expanded view of the hardware design in a Diya platform. Here, the light illumination source is an RGB LED matrix panel, an outdoor high refresh rate LED module containing 64x64 RGB LEDs with 3 mm pitch length. A computer cooling fan is attached to the back of the LED panel via a 3D printed back plate, which is custom-designed to guide air through vents ensuring proper air circulation behind the panel. The complete setup mounts on four 3D printed stands, which can be anchored to an incubator. Two standard multiwell plates with target cell cultures can be accommodated for simultaneous illumination on Diya platform. These plates are placed on top of custom-designed 3D printed adapters having holes underneath the individual wells. The adapters lock onto the desired position on the LED panel via carefully designed gridded protrusions underneath that can latch between LEDs on the panel. A light diffuser film/paper is sandwiched between the well plate and the adapter ensuring homogeneous illumination within a well region (Figures 2A and 2B). The adapters also ensure negligible light spillover between neighboring wells (Figure S2). The multiwell plates can be securely clamped down to the setup using a 3D printed adjustable clamping mechanism, if needed, for example in shaking incubators.

(B and C) (B) Diya communication channel (C) Diya operation protocol. First, the user configures/designs a light induction experiment on Diya GUI which generates the corresponding pattern file (.tif for static pattern, .gif for dynamic pattern). Then, using HDPlayer application the user sends the pattern file to the D16 receiving card over Wi-Fi. After saving the file locally, the card automatically starts transmitting the desired pattern to the panel which illuminates its LEDs accordingly.

For thermal management during light induction operation, we designed and implemented an active air circulation system. The system comprises a cooling fan attached on the back of the LED panel via a 3D-printed back plate (Figure 1A). This back plate is custom-designed with vents to allow proper air circulation behind the panel. This measure guarantees optimal dissipation of heat generated by LEDs and driver chips, mitigating any potential impact on the ambient temperature of the cell cultures that are cultivated on the Diya platform (Figure 2F). Given the low thermal conductivity of many 3D printing filaments, the 3D-printed well plate adapters serve as an effective insulation barrier, limiting the transfer of heat from the LED panel to the well plate and enhancing the thermal management strategy. The viability staining results displayed in Figure 2G demonstrate the effectiveness of the active air circulation mechanism on the Diya platform in maintaining a viable environment for cellular proliferation, even under the influence of strong light induction.

The Diya platform comprises commercially available and cost-effective components, as well as a few 3D-printed parts, resulting in a total cost of less than USD 200. A comprehensive list of components can be found in the Table S1. Assembly is straightforward and can be completed within an hour using basic tools, such as screwdrivers, without the need for specialized equipment. Additionally, the entire setup, including the well plates with target cell cultures, can be securely mounted within a humidified cell culture incubator with shaking capabilities for optimal cellular growth conditions (as depicted in Figure S3).

Enhancing user experience with the Diya GUI: Design and key features

The graphical user interface (GUI) for Diya provides a streamlined and intuitive interface for designing light induction experiments. The interface is designed to be user-friendly, eliminating the need for coding expertise and offering a wide range of customizable settings

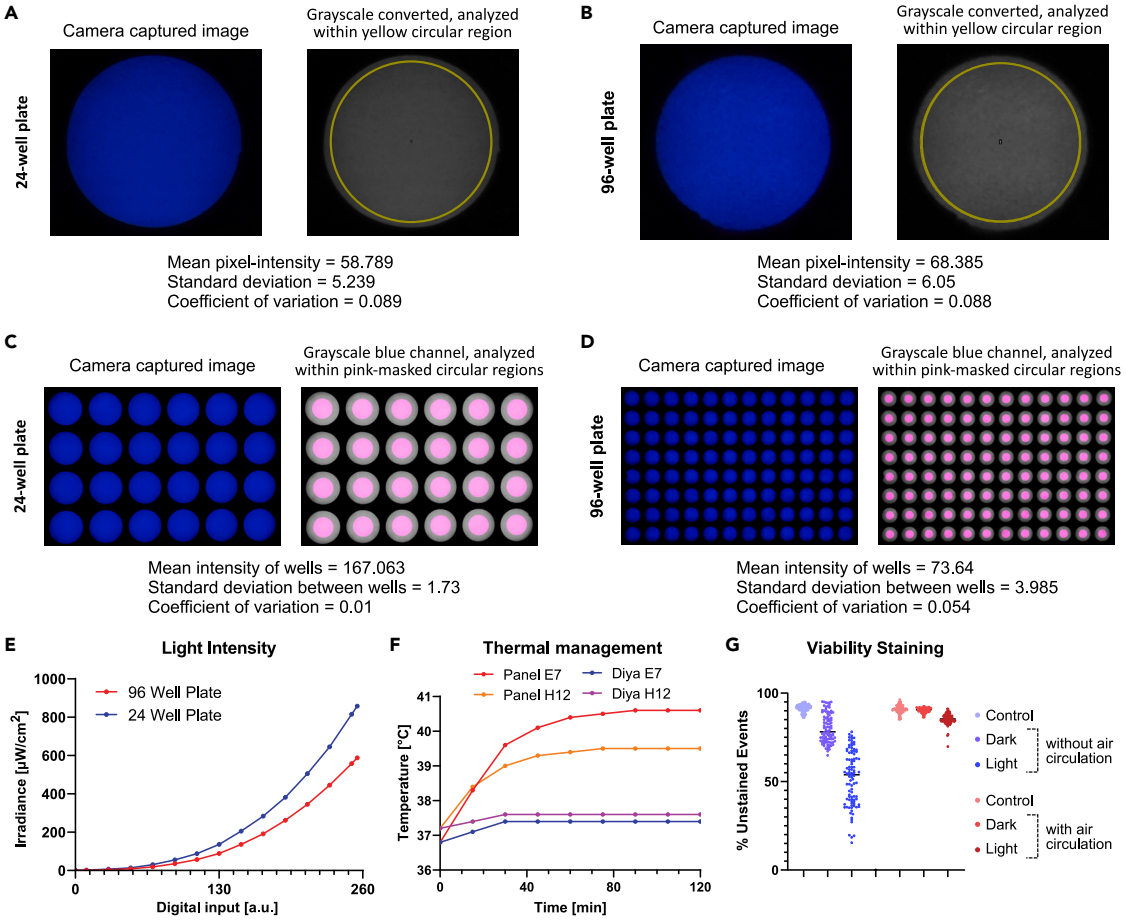

Figure 2. Diya characterization

(A and B) Single well (under illumination) images were captured and analyzed for homogeneity. First, the captured images were converted into grayscale format, and then a circular region, just lying within the well, was marked manually. ImageJ was used to compute mean pixel-intensity and standard deviation within the circular region. The coefficient of variation was observed to be less than 0.1 (in both 24- and 96-well plates) validating that each well receives homogeneous and uniform illumination on the Diya platform.

(C and D) With diffuser film placed on top of the well plate adapter, we captured photos of fully illuminated adapters (same digital input in all wells). Blue channel grayscale values were extracted for further analysis. Using MATLAB scripting, we created circular averaging masks (in pink) over all the wells. First, average pixel intensities within individual circular masks were computed, which were then used to calculate the mean and standard deviation of all masks. The coefficient of variation was observed to be less than 0.1 in both the 24-well and 96-well plate adapters. This implies that well-to-well light intensity variation is minimal in Diya platform.

(E) Light irradiance measured over a single illuminated well at different light inputs (digital levels). A well in a 24-well plate receives higher irradiance compared to that in a 96-well plate, possibly due to more illuminating LEDs per well.

(F) Measured temperature of liquid medium in two 96-well plates, first - directly placed on the LED matrix panel, and second - placed on the Diya platform with active air circulation system and well-plate adapter (Figure 1A), inside a humidified 37°C incubator. All 96 wells of the target plate were continuously illuminated with maximum light intensity. The thermal management system on the Diya platform robustly maintains the temperature below ~ 37.5°C, which can rise to over 40°C without the specially-designed adapters and active air circulation mechanism.

(G) Percentage of acquired unstained events observed in the flow cytometry measurements of all 96 cell (HEK293T) cultures in each of the six 96-well plates. The cells were stained with SYTOX™ Blue dead cell stain after 48 h of standard (humidified, 37°C, 5% CO2) cell culture incubation in three configurations. Here, the three 96-well plates with cells were placed directly on the incubator tray (Control), on the Diya platform with maximum intensity light illumination (Light), on the Diya platform without light next to the illuminated well plate (Dark). The same experiment was repeated twice - with and without active air circulation mechanism attached to the LED panel. The thermal management system on Diya platform provide viable conditions for cells under illumination to proliferate normally. Representative forward and side scatterplots can be viewed in Figure S8.

and layered functionalities. Users can easily create pattern files in either .tif or .gif format and upload them onto Diya to execute the desired light induction experiment.

The Diya GUI provides the user with the ability to configure experiments for 6-, 24-, or 96-well plates, and the capability to design simultaneous light induction experiments for two plates at the same time. The GUI enables independent selection of individual or groups of wells, and allows the user to choose from three color options (red with a wavelength of 622 nm, green with a wavelength of 520 nm, and blue with a

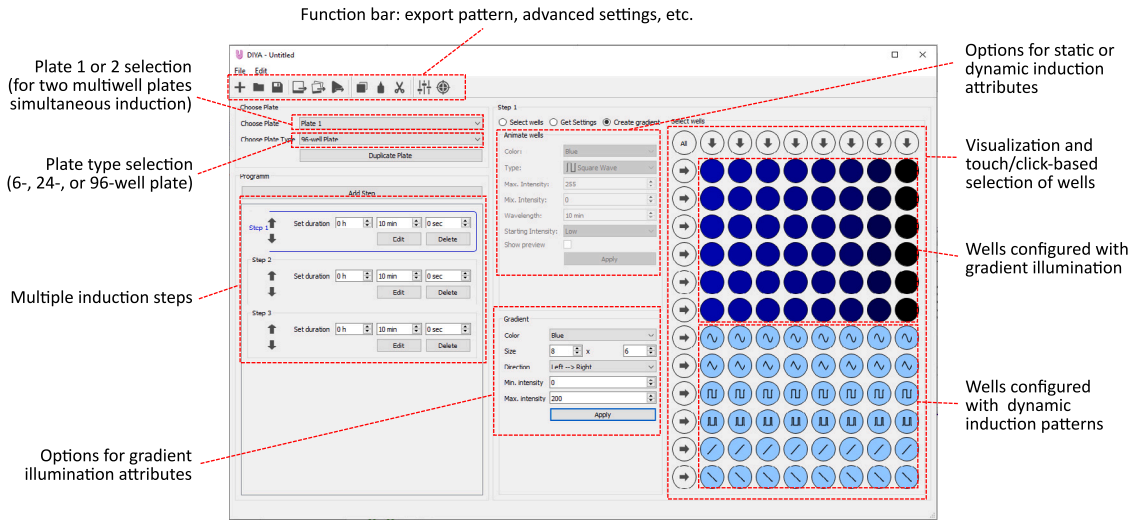

Figure 3. Diya GUI design

Different features and functionalities in Diya GUI.

wavelength of 464 nm) and set the desired light intensities for each, as illustrated in Figure 3. Furthermore, the GUI features a separate direct option for the user to define a desired intensity gradient for the selected group of wells, thus easing the process of designing dose response experiments for target *in vivo* process characterization. It also incorporates an elaborate option for designing time-varying dynamic induction experiments, providing the user with a set of six commonly used time-varying functions (sine wave, triangular wave, square wave, pulsed-width modulation (PWM), rising ramp, and falling ramp) and the ability to conveniently define parameters for each such as time-period of periodic inputs, maximum or minimum intensity, total induction time, and PWM duty cycle.

Inspired by the experiment design protocols proposed in Thomas et al.,[49] the Diya GUI organizes the light induction experiment as a multi-step induction process (Figure 3). The user can add, delete or modify any number of steps with different configurations. For example, one can design a 1 h constant light induction step, add another step with PWM induction for 1 h, and then a final step with 1 h rising ramp light induction. The three steps are automatically combined in a single pattern file (.gif format) which can be uploaded onto Diya for the desired multi-step experiment. By right-clicking on a well and selecting the "Information" option in the dropdown menu, the user can also visualize all the induction steps stitched together in a time plot with relevant details (Figure S7).

The Diya GUI offers the ability to design custom illumination patterns for well plates or culture dishes using its advanced settings option. The interface for designing custom patterns resembles a basic digital canvas drawing tool (as depicted in Figure S5). Furthermore, the built-in multiwell plate illumination patterns can be relocated to any preferred position on the panel via a touch/click interactive interface (as shown in Figure S6).

Once the configuration and induction steps for an experiment have been designed, the user can export the pattern file in .tif (for single-step constant light induction) or .gif (for multi-step time-varying light induction) format. For starting the experiment, this file can be uploaded to Diya over Wi-Fi using free HDPlayer application. The D16 receiving card stores the file in its onboard internal (4GB) memory and transmits the pattern to the LED panel for illumination whenever the setup is powered ON (Figure 1C). For .gif file generation (export option), the GUI first converts the induction steps into frames with a 1 FPS (by default) or user-defined FPS (frames per second) setting, and then uses a gif-converter toolbox to convert those frames into a single .gif file. For configuring a long-duration time-varying experiment, it is preferred to define a low FPS rate to speed up the frame conversion process.

Furthermore, we are working on adding more functionalities, such as a separate option to design pseudo-time course induction experiments, in future updates of our Diya GUI. Since the complete source code is openly available, any user with a coding know-how in python can themselves add/customize any further functions, if needed.

Performance characterization of Diya platform with different model organisms

After thoroughly evaluating the technical specifications of the Diya platform (as depicted in Figure 2), we performed extensive experiments to demonstrate the versatility and potential utility of our proposed device through the use of different optogenetic tools and genetic constructs in multiple model organisms. These experiments also demonstrate the operability of Diya under a variety of culturing conditions. To achieve this, we selected five widely used optogenetic tools (Opto-T7RNAP,[36] CcaS-CcaR,[23] EL222,[37] CRY2PHR-CIB1[38] and GAVPO[39]) in previously established bacterial, yeast, and human cell lines.

For *Escherichia coli*, we utilized a strain engineered with Opto-T7RNAP to expresses the mCherry fluorescent protein.[36] This tool consists of a split T7 RNA polymerase that is fused to the heterodimerizing Magnets, referred to as nMag and pMag, respectively. Upon exposure to blue light, the Magnets heterodimerize and reconstitute the T7RNAP, enabling the initiation of transcription of the fluorescent reporter

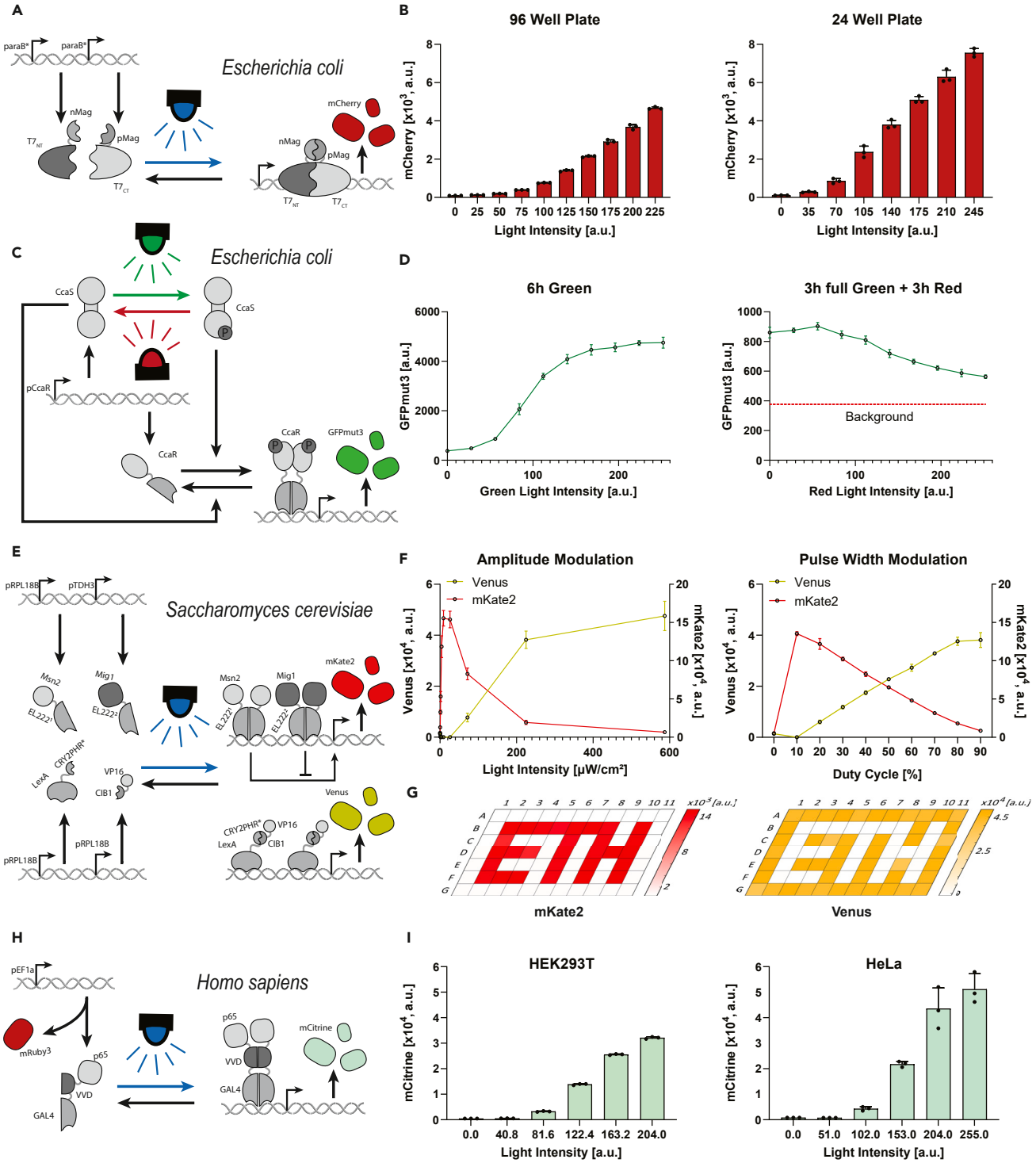

Figure 4. Diya characterization with optogenetic tools in model organisms

(A) An Opto-T7RNAP based circuit topology for light-dependent reporter expression in *E. coli*.[36]

(B) The fluorescent output of mCherry after 5 h of continuous induction with different blue light intensities. Experiments were performed with the Diya device with the target *E. coli* cells cultured in a 96- as well as 24-well plate.

(C) A CcaS-CcaR based circuit topology[23] for light-dependent reporter expression in *E. coli*. Green light illumination leads to the activation of this optogenetic system, while the natural dark reversion rate can be accelerated through red light illumination.

Figure 4. *Continued*

(D) Left panel: fluorescent output after 6 h of illumination with different intensities of green light. Right panel: fluorescent output after 3 h of green light induction at 252 a.u. intensity followed by 3 h of different red light intensities. The background fluorescence is shown as a dashed red line.

(E) Input light signal demultiplexer genetic circuit based on EL222 and CRY2PHR-CIB1 optogenetic tools in *S. cerevisiae*.[50] $EL222^1$ = EL222(AQT) $EL222^2$ = EL222(A79Q), CRY2PHR* = CRY2PHR(W349R).

(F) The expression levels of Venus and mKate2 fluorescent reporters after 6 h of continuous induction with sustained (constant) or pulsed (PWM) blue light inputs at different light intensities or duty cycles, respectively. In the pulsed light induction case, the ON time light illumination was performed with maximum light intensity value.

(G) In a 96-well plate culture with *S. cerevisiae* cell strain (described in (E)), wells forming ETH letters were illuminated with 10% duty-cycle while the other wells were kept at constant blue light induction for 6 h. Similar to the observed expression levels in (F), mKate2 showed predominant expression with pulsed light compared to constant light induction while Venus displayed an inverted expression pattern.

(H) A GAVPO-based circuit topology for light inducible mCitrine expression in human cell lines. The light inducible transcription factor GAVPO is encoded together with mRuby3 via a P2A linker.

(I) The fluorescent output of mCitrine for positively transfected HEK293T and HeLa cells with mRuby3, after 48 h of continuous blue light induction with different light intensities on the Diya platform. Experimental data are shown as the mean of 3 technical replicates and the standard deviation shown as error bars.

(Figure 4A). We conducted light intensity titration experiments using cells cultured in both a 96-well plate and a 24-well plate. To provide suitable growth conditions for the *E. coli* cell culture, the Diya platform and both culture well plates were secured inside a 37°C shaking incubator using the clamping safeguards available in the Diya design. In both well plates, after 5 h of continuous illumination, the reporter fluorescent intensity increased monotonically with the light intensity (Figure 4B), as previously described in Baumschlager et al.[36] The increased induction observed in the 24-well plate compared to the 96-well plate setup can be attributed to the higher light irradiance measured in the former plate, especially at high digital input values (Figure 2E).

Further demonstrating the induction feasibility with other LED wavelengths available on Diya platform, we used a previously published green-red optogenetic tool – CcaS-CcaR system (Figure 4C)[23] engineered in an *E. coli* strain. In this system, green light leads to the phosphorylation of CcaS *trans*-membrane protein, which activates its kinase properties and consequently transfers a phosphate group to CcaR molecule. Upon phosphorylation, the response element CcaR dimerizes, binds the promoter and initiates transcription of the fluorescent reporter gene GFPmut3. In the dark, CcaS reverts to its unphosphorylated state. This reversal process is accelerated with red light exposure. In our experiment, the cells were illuminated for 6 h at different green light intensities, resulting in an increased expression of fluorescent reporter with increasing light intensities. Expression saturation was observed at higher illumination intensities (Figure 4D, left). Red light illumination speeds up the natural dark dephosphorylation of CcaS.[23] The unphosphorylated CcaS acts as a phosphatase for CcaR. We illuminated the system with green light for 3 h at 252 a.u. intensity followed by 3 h of no light or illumination with different intensities of red light. This exhibited an increased inactivation rate in red light, which is reflected by lower levels of fluorescence output (Figure 4D, right).

For *Saccharomyces cerevisiae*, we selected a recently published strain engineered with a gene expression demultiplexer circuit,[50] which integrates two optogenetic tools: mutated variants of EL222[37] and CRY2PHR-CIB1,[38] and two fluorescent protein reporters Venus and mKate2. Depending on the dynamics (sustained or pulsed) of input light signals, this circuit design exhibits different reporter expression patterns, thus acting as a demultiplexer of input signals. Detailed information about the genetic constructs and their design considerations are available in Benzinger et al.[50] Briefly, the yellow fluorescent protein Venus is controlled by a LexA promoter. The DNA binding domain (DBD), LexA, is fused to CRY2PHR-CIB1(W349R). Upon blue light exposure, CRY2PHR-CIB1(W349R) can heterodimerize with CIB1, which is fused to the transcriptional activation domain (AD) VP16 (Figure 4E). The Venus reporter protein should therefore monotonically increase with the light intensity. The red fluorescent protein mKate2, on the other hand, is controlled by two mutated EL222 variants. EL222 homodimerizes upon blue light illumination and enables DNA binding to pEL222. One of the EL222 mutants, EL222(AQT), is fused to the Msn2 AD and has a slower reversion rate back to the inactive monomeric state. The other mutant EL222(A79Q) is fused to the repressing domain Mig1 and has a faster reversion rate. This genetic design forms a diamond incoherent feedforward loop toward the expression of mKate2 having parallel activation and repression pathways (Figure 4E). The faster reversion of the repressor compared to the activator leads to more mKate2 expression with pulsed light induction (PWM) and less expression with sustained high light intensity exposure. The expected expression patterns of Venus and mKate2 reporters were successfully reproduced after 6 h of PWM as well as constant light illumination with the Diya platform (Figure 4F).

In another experiment with the same *S. cerevisiae* strain mentioned above, we used 96-well plates for cell culture and created a pattern of pulsed (PWM) and constant light illumination in different wells using the Diya GUI. Here, wells forming the shape of ETH were illuminated with 10% duty cycle PWM light and the other wells received constant high intensity light induction. As expected, after 6 h of induction, mKate2 expression was predominantly observed in those ETH-forming wells compared to that in the rest of the wells, while Venus expression exhibited an inverted pattern (Figure 4G). This demonstrates the flexibility of Diya platform in handling both pulsed as well as sustained illumination patterns in one go, with robust optical isolation between neighboring wells. Similar to the setup in *E. coli* experiments, Diya platform and the illuminated well plates were clamped inside a 30°C shaking incubator to perform experiments with *S. cerevisiae*.

For the human cell lines, we used GAVPO in HEK293T and HeLa cells. GAVPO consists of the DBD GAL4, the light-inducible homodimerizing VVD domain and the AD p65. GAVPO was constitutively expressed together with fluorescent protein mRuby3 via a P2A linker (Figure 4H). Only cells that were expressing mRuby3 after the transient transfection were used in the analysis. Upon blue light illumination, GAVPO dimerizes, binds to the promoter and initiates transcription of the fluorescent reporter mCitrine. After 48 h of continuous illumination

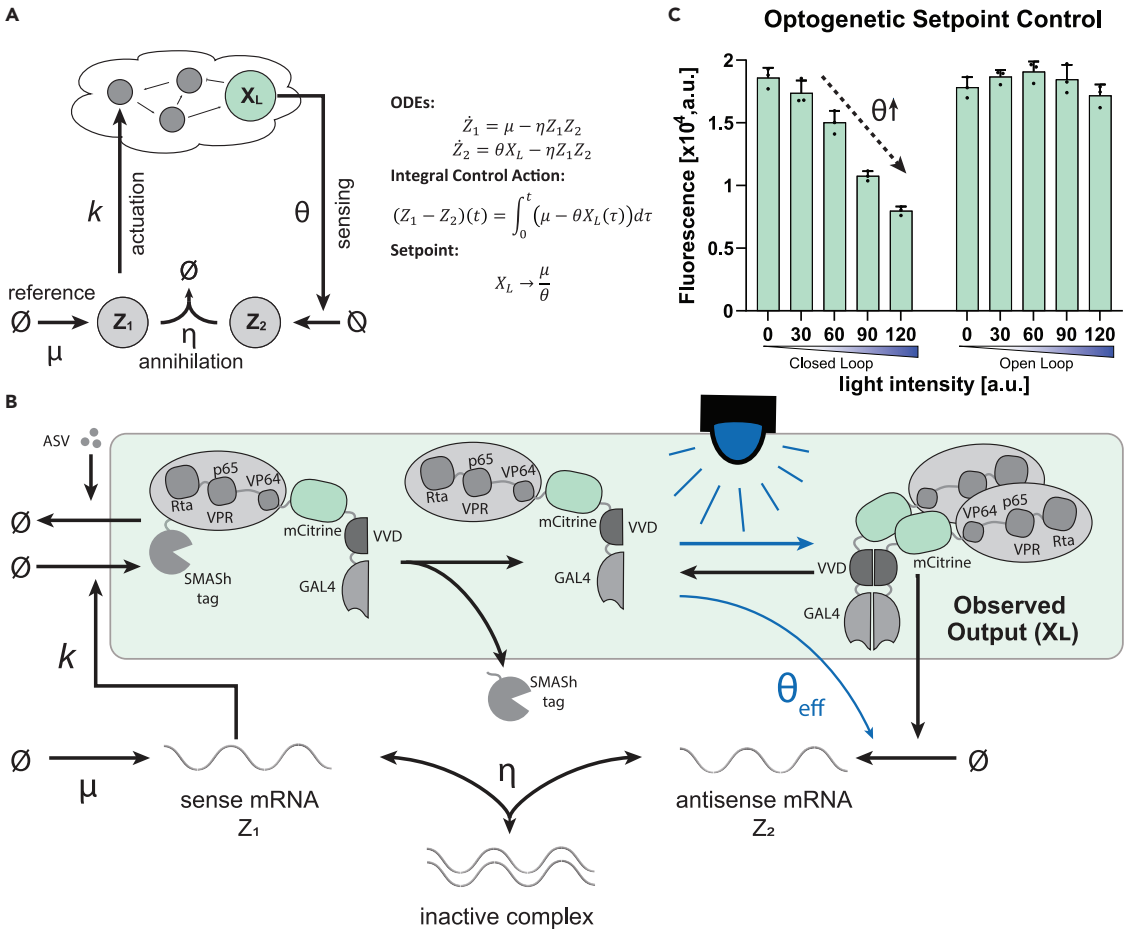

Figure 5. Diya application in advanced biomolecular controllers

(A) An illustration of AIF biomolecular controller reactions.[48] AIF motif involves four reactions (reference, actuation, sensing, and annihilation) with two controller species Z_1 and Z_2. Here, the output tracking set-point is determined by the reaction rates μ and θ.

(B) An *in vivo* implementation of the optogenetic AIF controller motif. This genetic design builds upon the *in vivo* controller engineered in mammalian cells by Frei et al.[42] with design modifications to make the sensing reaction light-inducible. Here, we used the optogenetic tool GAV-VPR that dimerizes into its active state upon blue light exposure. This active molecule then transcribes the antisense mRNA, which enables effective tuning of the sensing reaction rate (θ) using light. The observed output in this design is the sum of all GAV-VPR proteins independent of their dimerization status. The open-loop circuit, as mentioned in the text, does not have the antisense mRNA plasmid.

(C) This plot shows the output fluorescence compiled from 48 h continuous light induction titration experiments with our *in vivo* optogenetic AIF controller circuit using the Diya platform. Increasing the light intensity increases θ, which in turn decreases the output of interest, as it tries to track the set-point μ/θ. The open loop on the other hand is insensitive to the amount of light. Experimental data are shown as the mean of 3 technical replicates and the standard deviation shown as error bars.

on the Diya platform, both mammalian cell lines showed increasing mCitrine expression in response to increasing blue light induction intensities (Figure 4I). In these experiments, the Diya platform with illuminated well plates was placed in a humidified 37°C 5% CO_2 incubator.

The characterization experiments performed provide a clear demonstration of the Diya platform's capability to support the growth of different model organisms while inducing the desired response to light illumination. All of these results were consistent with expectations and provide compelling evidence of the full potential of this device.

Optogenetic set-point control

We further demonstrate an application of optogenetics and the use of Diya in the operation of advanced biomolecular controllers *in vivo*. In this regard, we have generated an *in vivo* optogenetic AIF controller. The AIF motif contains four biomolecular reactions (reference, sensing, actuation, and annihilation) involving two controller species Z_1 and Z_2 (Figure 5A).[48] Through the interplay of these reactions, the AIF motif drives the output molecule of interest (X_L) to track a set-point defined by the ratio of the reference reaction rate (μ) over the sensing gain (θ). This controller motif achieves the stated set-point tracking (with respect to output X_L) even in the presence of external disturbances and

parameter (except μ and θ) variations,[48] thus exhibiting robust perfect adaptation (RPA). The optogenetic AIF controller uses light as an input for reversibly adjusting the set-point without losing its RPA properties.

For our design we selected the recently published *in vivo* AIF motif designed in mammalian cells by Frei et al.[42] and modified one reaction to be light-inducible. This controller implementation consists of a sense mRNA ($\mathbf{Z}_1$) and its complementary antisense mRNA ($\mathbf{Z}_2$), which heterodimerize together and forms an inactive complex (annihilation reaction). The mRNA, being constitutively produced (reference reaction), translates (actuation reaction) the transcription factor (TF) tTA[51] fused to the mCitrine fluorophore and the asunaprevir (ASV) inducible degradation tag SMASh.[52] In our design, we exchanged the TF tTA for GAV-VPR,[39] an optogenetic tool. GAV-VPR consists of the truncated dimeric DNA binding domain (DBD) Gal4 (without the native dimerization domain), the light-inducible dimerizing domain VVD and the activation domain (AD) VPR. Upon blue light exposure, GAV-VPR dimerizes and initiates the transcription (sensing reaction) of the antisense mRNA ($\mathbf{Z}_2$), thus closing the feedback loop. The observed output ($\mathbf{X}_L$) in this circuit is the sum of all GAV-VPR molecules independent of their dimerization status. An illustration of this circuit design is shown in Figure 5B.

In this closed-loop scheme, blue light induction shifts the ratio of the observed output toward its active dimeric state, and thus determines the sensing reaction rate by governing θ. This also defines the output set-point (μ/θ, Figure 5A). We induced this *in vivo* circuit (transfected in HEK293T cells) with different blue light intensities continuously for 48 h on the Diya platform, and observed the steady-state mCitrine fluorescence (which is a proxy for the output molecule $\mathbf{X}_L$). The same induction experiment was performed with the same circuit but without the plasmid encoding the antisense mRNA; this removes the feedback pathway and acts as an open-loop system. As observed in Figure 5C, the output fluorescence at steady-state is negatively correlated with the input light intensity. This implies that the output set-point of our proposed optogenetic AIF circuit can indeed be varied by applying different light intensities. Moreover, this variation is not observed in the open-loop circuit design, which validates the working of our closed-loop implementation.

To further investigate our proposed circuit design, we performed another set of experiments with added ASV (asunaprevir) drug in the cell culture media. ASV emulates a disturbance source to the controller operation as it increases the degradation rate of newly formed GAV-VPR (Figure 5B). This results in a decrease in the steady-state output fluorescence which is evident in the open-loop case as shown in the Figure S1E. However, this disturbance was noticeably rejected in the closed-loop design, thus validating the RPA property of our proposed antithetic controller implementation (Figure S1). A compelling observation on the relationship between the degree of RPA and input light intensity, in the presence of biological limitations, is briefly discussed in the supplementary Section S2.

DISCUSSION

In this work, we designed a cell culture light illumination platform – Diya – compatible with multiwell plates and culture dishes. Owing to high density RGB LED matrix panel in its design, Diya enables light induction with three wavelengths (red, green and blue) in a plethora of different well plates or dishes of diverse shapes and sizes. With a multitude of optogenetic tools being developed and employed in different synthetic biology applications, there is a need for versatile illumination platforms capable of handling different experimental requirements. Diya incorporates many of those requirements in a single, easy-to-assemble, and user-friendly platform.

As the optogenetic applications are evolving over time, many studies demand targeting cell cultures with different light intensity profiles. In a recent study by Benzinger et al.,[50] it has been shown that one can induce different cellular responses by illuminating the culture with pulsed light profile vs. sustained constant light. Sustained light illumination at higher intensities results in excessive heat dissipation from LEDs and associated electronic components. Inspired from technologies previously demonstrated in the literature, Diya incorporates dedicated design elements for active air circulation in the setup, thus limiting the adverse thermal effects on the target cell culture under sustained illumination. The stable growth conditions bestowed by the Diya platform make it suitable for a wide range of model organisms and applications, as demonstrated in this work.

These optogenetic applications and tool-developments are mostly carried out in biology labs, which usually lack access to the necessary hardware and software engineering expertise and resources. Advanced light delivery platforms (such as microscope-coupled platforms[20]) are, in general, sophisticated machines, built on suitable optics, mechatronics and software technologies. Besides, they are also expensive to build and maintain, and offer limited throughput. These are major hurdles in expanding the use of optogenetic tools in various potential applications such as simple characterization and tool-optimization studies. Diya expands the inventory of high-throughput devices that embody inexpensive and simple hardware-software design elements. It is modular and easily serviceable, if needed, without requiring dedicated hardware engineering expertise and tools. Furthermore, one can design a wide variety of dynamic (time-varying) or static (constant) illumination experiments simply by clicking intuitive buttons provided on the Diya GUI without requiring any prior software training or coding skills. With the touch/click-based interactive interface, a user can choose different built-in well plate options, select individual or groups of wells for induction, decide light illumination intensities for selected wells, create gradient illumination patterns across selected wells, or design dynamic (e.g., sine wave, PWM, etc.) illumination patterns.

Although we targeted a given set of commonly-used multiwell plates in the design of Diya's peripherals, such as the plate-adapter, the modular hardware architecture of Diya allows one to easily exchange the dedicated parts without affecting the overall operation. In addition, the Diya GUI software has been developed with an open-source paradigm. If required, additional features can be incorporated into the GUI by easily appending and compiling the provided source code.

While developing various modalities of the Diya optogenetic platform, we also delved into the potential application of optogenetics in advanced biomolecular controller design. In this regard, we developed a light-controlled version of the RPA-achieving antithetic integral controller, and implemented the controller circuit in a human cell line. Using Diya as our light illumination device targeting our optogenetic

controller design, we demonstrated how one can vary the *in vivo* controller parameters by simply varying the light illumination intensity. This design can be applied for the rapid characterization of biomolecular controllers. Furthermore, we envision that such circuits will find widespread application in biotechnological or biomedical applications, which require robust temporal control over cellular processes. Optogenetic antithetic integral controllers such as the one proposed here could be applied in regulating stem cell differentiation, where certain morphogens have to be robustly maintained for a specific time window. Since light can be applied in a localized fashion, this light-inducible controller design methodology could be further employed in studies related to pattern formation and tissue engineering.

In conclusion, with Diya we aim to lower the entry barrier and bring optogenetics within a more accessible and affordable range for academic research labs, while not compromising with the quality standards of experimentation. It is worth emphasizing that Diya offers previously stated essential features while still being an easy-to-assemble and easy-to-use platform. The assembly parts of Diya are either inexpensive and readily available off-the-shelf components (LED panel and receiving card) or simple 3D-printable items (well plate adapter, panel back plate, and mounting parts). The assembly process requires minimal engineering expertise without needing any specialized tools or equipment. The intuitive GUI design renders the programming of light induction experiments an effortless and fun task requiring no coding skills. We strongly believe that these salient features associated with Diya deem it suitable for widescale adoption in biology labs pursuing optogenetics research.

Limitations of the study

Diya incorporates a modular and modifiable design, intended to be developed or modified further to cater to broader optogenetic applications. In this study, all the experiments were performed with 24- and/or 96-well plates. The well plate adapter designs provided in this paper are suited for the specific multiwell plate types mentioned in the STAR methods section. For any other culture plate, one needs to test and, if required, modify the well plate adapter design accordingly.

The core design element in our proposed Diya platform is the RGB LED matrix panel. This panel has fixed miniaturized RGB LEDs arranged in such a way that all three – red, green and blue – light sources are located within LED compartments (Figure S4). These LED compartments are distributed evenly in a 2-D grid with a 3 mm pitch between them. This pitch is suitable for multiwell plates with 96 (SBS standard format) or lower number of wells (having larger well diameter). Furthermore, it is not possible to change LEDs in these RGB LED panels. So, optogenetic induction experiments are limited to three fixed wavelengths (622, 520, and 464 nm). Although limited to fixed multiwell plate types, some other light induction devices, for example LPA,[31] offer the flexibility of exchanging LEDs, thus cater to wider optogenetic induction wavelengths. These devices can also be fitted with higher power LEDs providing higher induction intensities compared to that on Diya.

The Diya GUI is also developed as an open-source and easily updatable software. The current version of the software provided with this study does not incorporate a dedicated option for setting up pseudo-time course experiments, which could be useful in dynamic optogenetic induction studies. The frame rate for setting up dynamic induction profiles is fixed in the current version. This might lead to higher consumption of memory space while creating dynamic pattern files for longer duration experiments. One can easily compile the GUI software source code with a different frame rate value, if needed. We intend to add additional subtle features, and further improve the functionality of Diya GUI in future released versions.

STAR★METHODS

Detailed methods are provided in the online version of this paper and include the following:

- KEY RESOURCES TABLE
- RESOURCE AVAILABILITY
  - Lead contact
  - Materials availability
  - Data and code availability
- EXPERIMENTAL MODEL AND STUDY PARTICIPANT DETAILS
- METHOD DETAILS
  - Light intensity measurement
  - Temperature measurement
  - Plasmid construction
  - Mammalian cell culture (HEK293T and HeLa)
  - Transfection (HEK293T and HeLa)
  - Viability staining
  - Flow cytometry (HEK293T and HeLa)
  - Light induction experiment (*E. coli*)
  - Light induction experiment (*S. cerevisiae*)
- QUANTIFICATION AND STATISTICAL ANALYSIS
- ADDITIONAL RESOURCES
  - Diya - assembly instructions and GUI details

SUPPLEMENTAL INFORMATION

Supplemental information can be found online at https://doi.org/10.1016/j.isci.2023.107862.

ACKNOWLEDGMENTS

We thank Dr. Armin Baumschlager for help with characterization experiments involving the *E. coli* strain designed by him; Dr. Federica Cella and Dr. Sara Dionisi for performing some of the initial characterization experiments involving mammalian cells; Markus Klement for providing 3D printing and hardware workshop services; and Ellen Lau for providing services related to the LED panel purchase and operation. This project has received funding from the European Research Council (ERC) under the European Union's Horizon 2020 research and innovation programme (CyberGenetics; grant agreement no. 743269), and from a FET-Open research and innovation actions grant under the European Union's Horizon 2020 research and innovation programme (CyGenTiG; grant agreement no. 801041).

AUTHOR CONTRIBUTIONS

S.K. initiated the project and conceived the platform design idea. S.K. prototyped and designed the initial iterations and the final version of the Diya platform. S.K. and S.A. characterized the technical specifications. J.F. and S.K. designed the GUI. S.K.A. performed the *E. coli* experiments and proofread the manuscript. S.K. performed the *S. cerevisiae* experiments. C-H.C. and T.F. performed the HEK293T and the HeLa titrations, C-H.C. performed the viability staining experiment. S.A. designed the optogenetic AIF controller. S.A. performed the optogenetic AIF controller experiments and performed the data analysis. P.B. and P.A. provided workshop services and prototyped air circulation system. S.K. and S.A. wrote the first draft of the manuscript. M.K. contributed to the writing of the final draft of the manuscript, secured funding, and supervised the project.

DECLARATION OF INTERESTS

The authors declare no competing interests.

Received: March 28, 2023
Revised: July 25, 2023
Accepted: September 6, 2023
Published: September 9, 2023

REFERENCES

1. Toettcher, J.E., Voigt, C.A., Weiner, O.D., and Lim, W.A. (2011). The promise of optogenetics in cell biology: interrogating molecular circuits in space and time. Nat. Methods *8*, 35–38.
2. Deisseroth, K. (2011). Optogenetics. Nat. Methods *8*, 26–29.
3. Fracassi, C., Postiglione, L., Fiore, G., and Di Bernardo, D. (2016). Automatic control of gene expression in mammalian cells. ACS Synth. Biol. *5*, 296–302.
4. Müller, K., Naumann, S., Weber, W., and Zurbriggen, M.D. (2015). Optogenetics for gene expression in mammalian cells. Biol. Chem. *396*, 145–152.
5. Repina, N.A., Rosenbloom, A., Mukherjee, A., Schaffer, D.V., and Kane, R.S. (2017). At light speed: advances in optogenetic systems for regulating cell signaling and behavior. Annu. Rev. Chem. Biomol. Eng. *8*, 13–39.
6. Baumschlager, A., and Khammash, M. (2021). Synthetic Biological Approaches for Optogenetics and Tools for Transcriptional Light-Control in Bacteria. Adv. Biol. *5*, 2000256.
7. Gheorghiu, M., Polonschii, C., Popescu, O., and Gheorghiu, E. (2021). Advanced Optogenetic-Based Biosensing and Related Biomaterials. Materials *14*, 4151.
8. Pérez, A.L.A., Piva, L.C., Fulber, J.P., de Moraes, L.M., De Marco, J.L., Vieira, H.L., Coelho, C.M., Reis, V.C., and Torres, F.A. (2021). Optogenetic strategies for the control of gene expression in yeasts. Biotechnol. Adv. *54*, 107839.
9. Toettcher, J.E., Gong, D., Lim, W.A., and Weiner, O.D. (2011). Light control of plasma membrane recruitment using the Phy–PIF system. Methods Enzymol. *497*, 409–423.
10. Kolar, K., Knobloch, C., Stork, H., Žnidarič, M., and Weber, W. (2018). OptoBase: a web platform for molecular optogenetics. ACS Synth. Biol. *7*, 1825–1828.
11. Krueger, D., Izquierdo, E., Viswanathan, R., Hartmann, J., Pallares Cartes, C., and De Renzis, S. (2019). Principles and applications of optogenetics in developmental biology. Development *146*, dev175067.
12. McNamara, H.M., Ramm, B., and Toettcher, J.E. (2022). Synthetic developmental biology: New tools to deconstruct and rebuild developmental systems. In Seminars in Cell & Developmental Biology (Elsevier).
13. Carrasco-López, C., García-Echauri, S.A., Kichuk, T., and Avalos, J.L. (2020). Optogenetics and biosensors set the stage for metabolic cybergenetics. Curr. Opin. Biotechnol. *65*, 296–309.
14. Pouzet, S., Banderas, A., Le Bec, M., Lautier, T., Truan, G., and Hersen, P. (2020). The promise of optogenetics for bioproduction: dynamic control strategies and scale-up instruments. Bioengineering *7*, 151.
15. Sakar, M.S., Neal, D., Boudou, T., Borochin, M.A., Li, Y., Weiss, R., Kamm, R.D., Chen, C.S., and Asada, H.H. (2012). Formation and optogenetic control of engineered 3D skeletal muscle bioactuators. Lab Chip *12*, 4976–4985.
16. Hu, W., Li, Q., Li, B., Ma, K., Zhang, C., and Fu, X. (2020). Optogenetics sheds new light on tissue engineering and regenerative medicine. Biomaterials *227*, 119546.
17. Tian, C., Zhang, J., Gu, J., Li, W., and Cao, Y. (2022). Light controlled biomaterials for regulating cell migration and differentiation. Smart Materials in Medicine *3*, 209–216.
18. Reshetnikov, V.V., Smolskaya, S.V., Feoktistova, S.G., and Verkhusha, V.V. (2022). Optogenetic approaches in biotechnology and biomaterials. Trends Biotechnol. *40*, 858–874.
19. Kumar, S., Rullan, M., and Khammash, M. (2021). Rapid prototyping and design of cybergenetic single-cell controllers. Nat. Commun. *12*, 5651–5713.
20. Kumar, S., and Khammash, M. (2022). Platforms for optogenetic stimulation and feedback control. Front. Bioeng. Biotechnol. *10*, 918917.
21. Chait, R., Ruess, J., Bergmiller, T., Tkačik, G., and Guet, C.C. (2017). Shaping bacterial population behavior through computer-interfaced control of individual cells. Nat. Commun. *8*, 1535–1611.
22. Rullan, M., Benzinger, D., Schmidt, G.W., Milias-Argeitis, A., and Khammash, M. (2018). An optogenetic platform for real-time, single-cell interrogation of stochastic transcriptional regulation. Mol. Cell *70*, 745–756.e6.
23. Milias-Argeitis, A., Rullan, M., Aoki, S.K., Buchmann, P., and Khammash, M. (2016). Automated optogenetic feedback control for precise and robust regulation of gene expression and cell growth. Nat. Commun. *7*, 12546.

24. Steel, H., Habgood, R., Kelly, C.L., and Papachristodoulou, A. (2020). In situ characterisation and manipulation of biological systems with Chi. Bio. PLoS Biol. *18*, e3000794.
25. Pen, U.-Y., Nunn, C.J., and Goyal, S. (2021). An automated tabletop continuous culturing system with multicolor fluorescence monitoring for microbial gene expression and long-term population dynamics. ACS Synth. Biol. *10*, 766–777.
26. Lalwani, M.A., Zhao, E.M., and Avalos, J.L. (2018). Current and future modalities of dynamic control in metabolic engineering. Curr. Opin. Biotechnol. *52*, 56–65.
27. Lalwani, M.A., Ip, S.S., Carrasco-López, C., Day, C., Zhao, E.M., Kawabe, H., and Avalos, J.L. (2021). Optogenetic control of the lac operon for bacterial chemical and protein production. Nat. Chem. Biol. *17*, 71–79.
28. Zhao, E.M., Lalwani, M.A., Chen, J.-M., Orillac, P., Toettcher, J.E., and Avalos, J.L. (2021). Optogenetic amplification circuits for light-induced metabolic control. ACS Synth. Biol. *10*, 1143–1154.
29. Chen, M., Mertiri, T., Holland, T., and Basu, A.S. (2012). Optical microplates for high-throughput screening of photosynthesis in lipid-producing algae. Lab Chip *12*, 3870–3874.
30. Müller, K., Zurbriggen, M.D., and Weber, W. (2014). Control of gene expression using a red-and far-red light–responsive bi-stable toggle switch. Nat. Protoc. *9*, 622–632.
31. Gerhardt, K.P., Olson, E.J., Castillo-Hair, S.M., Hartsough, L.A., Landry, B.P., Ekness, F., Yokoo, R., Gomez, E.J., Ramakrishnan, P., Suh, J., et al. (2016). An open-hardware platform for optogenetics and photobiology. Sci. Rep. *6*, 35363–35413.
32. Hennemann, J., Iwasaki, R.S., Grund, T.N., Diensthuber, R.P., Richter, F., and Möglich, A. (2018). Optogenetic control by pulsed illumination. Chembiochem *19*, 1296–1304.
33. Bugaj, L.J., and Lim, W.A. (2019). High-throughput multicolor optogenetics in microwell plates. Nat. Protoc. *14*, 2205–2228.
34. Repina, N.A., McClave, T., Johnson, H.J., Bao, X., Kane, R.S., and Schaffer, D.V. (2020). Engineered illumination devices for optogenetic control of cellular signaling dynamics. Cell Rep. *31*, 107737.
35. Höhener, T.C., Landolt, A.E., Dessauges, C., Hinderling, L., Gagliardi, P.A., and Pertz, O. (2022). LITOS-a versatile LED illumination tool for optogenetic stimulation. Sci. Rep. *12*, 13139.
36. Baumschlager, A., Aoki, S.K., and Khammash, M. (2017). Dynamic blue light-inducible T7 RNA polymerases (Opto-T7RNAPs) for precise spatiotemporal gene expression control. ACS Synth. Biol. *6*, 2157–2167.
37. Motta-Mena, L.B., Reade, A., Mallory, M.J., Glantz, S., Weiner, O.D., Lynch, K.W., and Gardner, K.H. (2014). An optogenetic gene expression system with rapid activation and deactivation kinetics. Nat. Chem. Biol. *10*, 196–202.
38. Taslimi, A., Zoltowski, B., Miranda, J.G., Pathak, G.P., Hughes, R.M., and Tucker, C.L. (2016). Optimized second-generation CRY2–CIB dimerizers and photoactivatable Cre recombinase. Nat. Chem. Biol. *12*, 425–430.
39. Wang, X., Chen, X., and Yang, Y. (2012). Spatiotemporal control of gene expression by a light-switchable transgene system. Nat. Methods *9*, 266–269.
40. Tabor, J.J., Levskaya, A., and Voigt, C.A. (2011). Multichromatic control of gene expression in Escherichia coli. J. Mol. Biol. *405*, 315–324.
41. Anastassov, S., Filo, M., Chang, C.-H., and Khammash, M. (2023). A cybergenetic framework for engineering intein-mediated integral feedback control systems. Nat. Commun. *14*, 1337.
42. Frei, T., Chang, C.-H., Filo, M., Arampatzis, A., and Khammash, M. (2022). A genetic mammalian proportional–integral feedback control circuit for robust and precise gene regulation. Proc. Natl. Acad. Sci. USA *119*, e2122132119.
43. Aoki, S.K., Lillacci, G., Gupta, A., Baumschlager, A., Schweingruber, D., and Khammash, M. (2019). A universal biomolecular integral feedback controller for robust perfect adaptation. Nature *570*, 533–537.
44. Filo, M., Kumar, S., and Khammash, M. (2022). A hierarchy of biomolecular proportional-integral-derivative feedback controllers for robust perfect adaptation and dynamic performance. Nat. Commun. *13*, 2119.
45. Ng, A.H., Nguyen, T.H., Gómez-Schiavon, M., Dods, G., Langan, R.A., Boyken, S.E., Samson, J.A., Waldburger, L.M., Dueber, J.E., Baker, D., and El-Samad, H. (2019). Modular and tunable biological feedback control using a de novo protein switch. Nature *572*, 265–269.
46. Huang, H.-H., Qian, Y., and Del Vecchio, D. (2018). A quasi-integral controller for adaptation of genetic modules to variable ribosome demand. Nat. Commun. *9*, 5415–5512.
47. Jones, R.D., Qian, Y., Ilia, K., Wang, B., Laub, M.T., Del Vecchio, D., and Weiss, R. (2022). Robust and tunable signal processing in mammalian cells via engineered covalent modification cycles. Nat. Commun. *13*, 1720–1817.
48. Briat, C., Gupta, A., and Khammash, M. (2016). Antithetic integral feedback ensures robust perfect adaptation in noisy biomolecular networks. Cell Syst. *2*, 15–26.
49. Thomas, O.S., Hörner, M., and Weber, W. (2020). A graphical user interface to design high-throughput optogenetic experiments with the optoPlate-96. Nat. Protoc. *15*, 2785–2787.
50. Benzinger, D., Ovinnikov, S., and Khammash, M. (2022). Synthetic gene networks recapitulate dynamic signal decoding and differential gene expression. Cell Syst. *13*, 353–364.e6.
51. Gossen, M., and Bujard, H. (1992). Tight control of gene expression in mammalian cells by tetracycline-responsive promoters. Proc. Natl. Acad. Sci. USA *89*, 5547–5551.
52. Chung, H.K., Jacobs, C.L., Huo, Y., Yang, J., Krumm, S.A., Plemper, R.K., Tsien, R.Y., and Lin, M.Z. (2015). Tunable and reversible drug control of protein production via a self-excising degron. Nat. Chem. Biol. *11*, 713–720.
53. Lee, M.E., DeLoache, W.C., Cervantes, B., and Dueber, J.E. (2015). A highly characterized yeast toolkit for modular, multipart assembly. ACS Synth. Biol. *4*, 975–986.

STAR★METHODS

KEY RESOURCES TABLE

REAGENT or RESOURCE	SOURCE	IDENTIFIER
Bacterial and virus strains		
E. coli BW25113 *attB::lacYA177C-kanR*(AB360); *PlacI-lacI-PT7- mCherry-ColE1-ampR* (pAB50,Addgene#101678);*ParaB*-T7RNAP1-563::GGSGG::nMagHigh1-rrnBT1-ParaB*—T7g10(5′UT R) - pMag::GGSGG::T7RNAP(R632S)564-883-pSC101-camR* (pAB150,Addgene #101661)	Baumschlager et al.[36]	AB363
E. coli JT2 Δ*metE::FRT Tn7::FRT-PcpcG2Δ59-metE, kanR* (SKA974, Addgene #80381); *PcpcG2Δ59 RBS3-gfpmut3-PccaR RBS-ccaR::FLAG-ccaS::FLAGColE1-camR* (pSKA413, Addgene #80403); *Plac/ara—1-ho1-pcyA-specR* (pPLPCB(S))	Milias-Argeitis et al.[23]; Tabor et al.[40]	SKA988
S. cerevisiae BY4741;his3Δ::pr5xBS-CYC180-Kozak-mKate2-tADH1t-HIS3MX (pDB60); *URA3::prRPL18B-Msn2AD-EL222*(AQT)*-tENO2; prTDH3-Mig1RDEL222*(A79Q)*-tPGK1(pYTKmk90); LEU2::prRPL18B-VP16AD-CIB1- tPGK1–prRPL18B-LexA-CRY2PHR*(W349R)*-tENO2–prLexACYCmin - Venus-tADH1*(pSO41)	Benzinger et al.[50]	DBY183
Experimental models: Cell lines		
HEK293T	ATCC	CRL-3216
HeLa	ATCC	CCL-2
Recombinant DNA		
EF1a GAV-VPR-mCitrine-SMASh lateSV40polyA	This laboratory	SA31
5xpUAS inverse(GAV-VPR-mCitrine-SMASh) lateSV40polyA	This laboratory	SA47
pUAS mCitrine lateSV40polyA	This laboratory	CH322
EF1a GAVPO P2A mRuby3 lateSV40polyA	This laboratory	CH607
empty backbone	This laboratory	GLM171
EF1a miRFP670 lateSV40polyA	This laboratory	TF138
Software and algorithms		
Diya GUI	This study	https://github.com/santkumar/diya
Other		
64x64 P3 outdoor full color LED module (Coreman)	Alibaba	N/A
LED module/panel AC/DC power adapter (5V, 10A)	DigiKey	1528-1519-ND
Power connector for LED panel (female 5.5 mm, 2.1 mm axial)	Conrad	TC-7227460
HD-D16 receiving card (HUIDU)	Alibaba	N/A
Receiving card AC/DC power adapter (5V, 1A)	Farnell	VEL05US050-EU-JA
Wired power connector for receiving card (female 5.5 mm, 2.1 mm axial)	Conrad	072062
DC cooling fan 5V	Distrelec	109R0605H402
Screws - M4, length 20 mm, head diameter <8 mm	Distrelec	BN 610 M4X20MM
Screws - M4, length 35 mm, head diameter <8 mm	Digitec	94574

(*Continued on next page*)

Continued

REAGENT or RESOURCE	SOURCE	IDENTIFIER
Wing or butterfly screws - M4, thread length 20 mm	SFS	151884
Standard hexagonal nuts - M4	Bossard	BN 630
Back plate	3D printed	N/A
Well plate adapter (3D printed)	3D printed	N/A
Stands (3D printed)	3D printed	N/A
Well plate clamper (3D printed)	3D printed	N/A
Side clamps (3D printed)	3D printed	N/A

RESOURCE AVAILABILITY

Lead contact

Further information and requests for resources and reagents should be directed to and will be fulfilled by the lead contact, Mustafa Khammash (mustafa.khammash@bsse.ethz.ch).

Materials availability

Plasmids generated in this study are available on request.

Cell lines generated in this study are available on request.

This study did not generate new unique reagents.

A complete assembly instruction together with related design files are available in this GitHub repository: https://github.com/santkumar/diya.

Data and code availability

- All reported data in this paper will be shared by the lead contact upon request.
- All original code has been deposited at GitHub repository (https://github.com/santkumar/diya) and is publicly available as of the date of publication. The Diya GUI URL is listed in the key resources table.
- Any additional information required to reanalyze the data reported in this paper is available from the lead contact upon request.

EXPERIMENTAL MODEL AND STUDY PARTICIPANT DETAILS

HEK293T (ATCC, strain number CRL-3216) and HeLa (ATCC, strain number CCL-2) cells were grown in Dulbecco's modified Eagle's medium (DMEM) supplemented with 10% FBS, 1x GlutaMAX, 1 mm Sodium Pyruvate, penicillin (100 U/μL), and streptomycin (100 μg/mL) at 37° C with 5% CO_2. The cell culture was detached with Trypsin-EDTA and split every 2 to 3 days into a fresh T25 flask. The cell suspension generated during the passaging was used for the transfection.

Escherichia coli cells were grown in M9 medium supplemented with 0.2% casamino acids, 0.4% glucose, 0.001% thiamine, 0.00006% ferric citrate, 0.1 mM calcium chloride, 1 mM magnesium sulfate, and 20 μg/mL uracil, and incubated in an environmental shaker at 37°C with shaking at 230 rpm. Antibiotics were used at the following concentrations: ampicillin (amp), 100 μg/mL; kanamycin (kan), 40 μg/mL; chloramphenicol (cam), 34 μg/mL; spectinomycin (spec), 100 μg/mL.

Saccharomyces cerevisiae cells were grown in synthetic medium (SD, LOFLO yeast nitrogen base, 5 g/L ammonium sulfate, 2% glucose, and pH adjusted to 6.0), and incubated in an environmental shaker at 30°C with shaking at 180 rpm.

METHOD DETAILS

Light intensity measurement

Light irradiance, reported in Figure 2E, was measured by using a microscope slide photodiode sensor (S170C, Thorlabs) with a power meter interface (PM100USB, Thorlabs). One well of the 96- or 24-well plate adapter was illuminated with different light inputs (digital levels). The corresponding irradiance was measured by placing the photodiode sensor face down (sensing area facing the adapter well) on top of the adapter with a diffuser film sandwiched in between.

Temperature measurement

Temperature measurements in Figure 2F were taken by using a sensitive thermometer (Greisinger G1202-GTF300). All wells of a 96-well plate were filled with DMEM medium, and the plate was then placed either directly on the LED matrix panel (power unplugged) or on the unplugged Diya platform (LED panel attached with the proposed thermal management system) inside a humidified 37°C cell culture incubator. The two wired thermometer probes were carefully dipped in the medium in wells E7 (center) and H12 (corner) of the well plate. The incubator

door was closed with the thermometer wires passing through the door rubber seal and connecting to the display module outside. The setup was left untouched for 2 h for the temperature of the medium in the well-plate to stabilize around 37°C (incubation temperature). After 2 h of incubation, the LED panel was plugged in and all the wells were illuminated with maximum light intensity. Measurements from two probes were recorded manually every 15 min for the next 2 h.

Plasmid construction

A mammalian adaptation of the modular cloning (MoClo) yeast toolkit standard[53] was used for assembling the gene fragments into plasmids. The individual gene fragments were amplified by PCR (Phusion Flash High-Fidelity PCR Master Mix; Thermo Scientific). All enzymes used in the golden gate assembly were obtained from New England Biolabs (NEB). The plasmids were chemically transformed into *E. coli* Top10 strains and isolated using ZR Plasmid Miniprep-Classic (Zymo Research). A list of all plasmids can be view in the Table S3.

Mammalian cell culture (HEK293T and HeLa)

HEK293T (ATCC, strain number CRL-3216) and HeLa (ATCC, strain number CCL-2) cells were grown in Dulbecco's modified Eagle's medium (DMEM; Gibco) supplemented with 10% FBS (Sigma-Aldrich), 1x GlutaMAX (Gibco), 1 mm Sodium Pyruvate (Gibco), penicillin (100 U/μL), and streptomycin (100 μg/mL) (Gibco) at 37° with 5% CO_2. The cell culture was detached with Trypsin-EDTA (Gibco) and split every 2 to 3 days into a fresh T25 flask (Axon Lab). The cell suspension generated during the passaging was used for the transfection.

Transfection (HEK293T and HeLa)

The cell density within the cell suspension was obtained with the automated cell counter Countess II FL (Invitrogen). 26'000 cells were seeded with a volume of 100 μL DMEM (lacking penicillin and streptomycin) in each well of the black CELLSTAR 96 well μClear plate (Greiner). For the AIF controller experiments, the medium contained in addition 11 nM Asunaprevir dissolved in DMSO (Sigma-Aldrich) (disturbed) or the equivalent amount of DMSO. After 24 h the HEK293T cells were transfected with a Polyethylenimine (PEI) "MAX" (MW 40000; Polysciences, Inc.) at a 1:3 (μg DNA to μg PEI) ratio in Opti-MEM I (Gibco). The HeLa cells were transfected with Lipofectamine 2000 (Thermo Fisher Scientific) at a 1:3 (μg DNA to μL Lipofectamine 2000) ratio in Opti-MEM I (Gibco). The transfection mixture was incubated for about 20 min and then 10 μL with a total of 100 ng of DNA were transferred per well. After the transfection, the plate was immediately put on the Diya. The transfection tables can be found in the Tables S4 and S5.

Viability staining

After 48 h of continuous light induction on Diya, cells were washed by PBS and detached in 53 μL Accutase solution (Sigma-Aldrich) containing 1 μM SYTOX™ Blue dead cell stain (Thermo Fisher Scientific) per well and put on the Eppendorf ThermoMixer C at 25 °C at 700 rpm for 20 min (Figure 2G). The data collection was performed on the Beckman Coulter CytoFLEX S flow cytometer with the 405 nm excitation with a 450/45 bandpass filter. The data was processed on the CytExpert 2.3 software.

Flow cytometry (HEK293T and HeLa)

After 48 h of continuous light induction on Diya, cells were detached with 53 μL Accutase solution (Sigma-Aldrich) per well and put on the Eppendorf ThermoMixer C at 25 °C at 700 rpm for 20 min. The data collection was performed on the Beckman Coulter CytoFLEX S flow cytometer with the 488 nm excitation with a 525/40+OD1 bandpass filter and the 638 nm excitation with a 660/10 bandpass filter. The data was processed on the CytExpert 2.3 software.

Light induction experiment (*E. coli*)

Escherichia coli cells were grown in M9 medium supplemented with 0.2% casamino acids, 0.4% glucose, 0.001% thiamine, 0.00006% ferric citrate, 0.1 mM calcium chloride, 1 mM magnesium sulfate, and 20 μg/mL uracil (Sigma-Aldrich Chemie GmbH), and incubated in an environmental shaker (New Brunswick) at 37°C with shaking at 230 rpm. Antibiotics (Sigma-Aldrich Chemie GmbH) were used at the following concentrations: ampicillin (amp), 100 μg/mL; kanamycin (kan), 40 μg/mL; chloramphenicol (cam), 34 μg/mL; spectinomycin (spec), 100 μg/mL.

E. coli strain AB363 (Opto-T7RNAP system and mCherry fluorescent protein reporter,[36] (Table S2) was used for the blue light induction titration experiment. A 5 mL aliquot of M9 medium (containing appropriate antibiotics) in a light-proof tube (Greiner, #188280) was inoculated with AB363 from a glycerol freeze stock. The culture was incubated overnight in the dark to stationary phase at 37°C, 230 rpm. The overnight culture was diluted 1:20,000 into fresh M9 medium immediately before starting the experiment. Diluted cells were induced with light in either a black, clear bottom 96-well plate (μClear CELLSTAR, Greiner, #655090) or a black, clear bottom 24-well plate (PerkinElmer, #1450-606) and sealed with a BREATHseal film (Greiner) and plastic lid. 200 μL of culture was incubated per well of the 96-well plate and one mL of culture was incubated per well of the 24-well plate. Cultures were induced with constant blue light (464 nm) at different intensities for 5 h (37°C, 230 rpm) before stopping transcription and translation with rifampicin and tetracycline and maturing the mCherry reporter as previously described.[36] mCherry fluorescence was measured on a CytoFlex S flow cytometer (Beckman Coulter) with a 561 nm laser and 610/20 band-pass filter; the gain settings were as follows: forward scatter 100, side scatter 100, mCherry 300. Thresholds of 2,500 FSC-H and 1,000 SSC-H were used for all samples. At least 50,000 events were recorded and cells were manually gated on an FSC- H/SSC-H plot corresponding to the experimentally

determined size of the testing strain at logarithmic growth and was kept constant for analysis of all samples using CytExpert Software (Beckman Coulter).

E. coli strain SKA988 (CcaS-CcaR system and GFPmut3 fluorescent protein reporter, Table S2)[23] was used for the red/green light induction titration experiment. For this system, it is important that the cells are kept in exponential phase both before and during light induction. A 5 mL aliquot of M9 medium (containing appropriate antibiotics) in a light-proof tube was inoculated with SKA988 from a glycerol freeze stock at a starting optical density at 600 nm (OD600) of $2x10^{-8}$. The culture was incubated overnight in the dark at 37°C, 230 rpm for 10.5 h to an OD600 lower than 0.1. The exponential phase culture was then diluted to an OD600 of 0.00001 in fresh M9 medium immediately before starting the light induction experiment. Diluted cells were induced with light in a black, clear bottom 96-well plate (200 μL culture per well) and sealed with a BREATHseal film and plastic lid. Cultures were incubated at 37°C, 230 rpm and induced with 6 h of constant green light (520 nm) at different intensities or with 3 h of constant green light with an intensity of 252 a.u. followed by 3 h of constant red light (622 nm) at different intensities. After 6 h of illumination, transcription and translation was stopped with rifampicin and tetracycline[36] and GFPmut3 was matured for 1 h at 37°C. GFPmut3 fluorescence was measured on a CytoFlex S flow cytometer (Beckman Coulter) with a 488 nm laser and 525/40 bandpass filter; the gain settings were as follows: forward scatter 100, side scatter 100, GFPmut3 100. Thresholds of 2,500 FSC-H and 1,000 SSC-H were used for all samples. At least 50,000 events were recorded and cells were manually gated on an FSC-H/SSC-H plot corresponding to the experimentally determined size of the testing strain at logarithmic growth and was kept constant for analysis of all samples using CytExpert Software (Beckman Coulter).

Light induction experiment (*S. cerevisiae*)

Saccharomyces cerevisiae cells were grown in synthetic medium (SD, LOFLO yeast nitrogen base (ForMedium), 5 g/L ammonium sulfate, 2% glucose, and pH adjusted to 6.0). A previously-published *S. cerevisiae* strain DBY183 (Table S2)[50] was used in the light amplitude and pulse-width modulation experiments. Cell culture in 3 mL fresh medium were started from glycerol freeze stock and grown overnight in a light-proof tube (Greiner, #188280) placed in a shaking (180 RPM) 30°C incubator. The OD600 was maintained lower than 0.4. Before starting the experiment, the overnight cultures were diluted to an OD600 of 0.01 using fresh SD medium, and 200 μL of the diluted culture was pipetted in each well of black, clear bottom 96-well plate (μClear CELLSTAR, Greiner, #655090). The plate was then placed on the Diya platform, and blue light (464 nm) illumination with different intensities or different pulsed-width modulation duty cycle was started immediately. After 6 h of illumination, cell samples were collected and incubated in SD medium with 0.1 mg/mL cycloheximide for 3 h in 30°C incubator.[50] This allowed full maturation of the fluorescent proteins *in vivo*. All the samples were then analyzed using a CytoFlex S flow cytometer (Beckman Coulter) for RFP (561 nm exciation laser and 585/42 emission filter) and YFP (488 nm excitation laser and 525/40 emission filter) fluorescence intensities. Following gain settings were used: forward scatter 100, side scatter 100, YFP 82, RFP 145. At least 2000 events were recorded and cells were manually gated on forward scatter vs. side scatterplot as described in Benzinger et al.[50] Gated cells were analyzed for mean and standard deviation values using CytExpert Software (Beckman Coulter). For qualitative plotting (Figure 4F), negative mean values (due to default instrument corrections) were replaced with zeroes.

QUANTIFICATION AND STATISTICAL ANALYSIS

Details of statistical analysis are mentioned in the corresponding figure legends. Data represent mean ± standard deviation.

ADDITIONAL RESOURCES

Diya - assembly instructions and GUI details

All design files and detailed instructions for assembling a Diya platform are provided in the GitHub repository: https://github.com/santkumar/diya. GUI stable releases and source codes are also maintained in the same repository.